

# Finite Conductivity in Mesoscopic Hall Bars of Inverted InAs/GaSb Quantum Wells

Ivan Knez\* and R.R. Du

*Department of Physics and Astronomy, Rice University, Houston, TX 77251-1892*

Gerard Sullivan

*Teledyne Scientific and Imaging, Thousand Oaks, CA*

We have studied experimentally the low temperature conductivity of mesoscopic size InAs/GaSb quantum well Hall bar devices in the inverted regime. Using a pair of electrostatic gates we were able to move the Fermi level into the electron-hole hybridization state, and observe a mini gap. Temperature dependence of the conductivity in the gap shows residual conductivity, which can be consistently explained by the contributions from the free as well as the hybridized carriers in the presence of impurity scattering, as proposed by Naveh and Laikhtman [Euro. Phys. Lett., 55, 545-551 (2001)]. Experimental implications for the stability of proposed helical edge states will be discussed.

It was recently proposed by Kane and Mele<sup>1</sup>, and independently, by Bernevig and Zhang<sup>2</sup> that a novel transport phenomenon, termed the quantum spin Hall effect (QSHE) should arise in a class of two-dimensional topological insulators (TI). The QSHE phase is characterized by an odd number of Kramer pair states at the edges, and an insulating gap in the bulk. Edge states are robust against disorder due to the topology of the bands and result in helical edge transport with counter-propagating spin-up and spin-down channels. Four-probe transport measurements on such structures at zero magnetic field give a near quantized conductance of  $2e^2/h$  for mesoscopic samples. Just as theoretically predicted by Bernevig et al<sup>3</sup>, the QSHE was soon observed in HgTe/CdTe quantum wells<sup>4</sup>. More recently, Liu et al<sup>5</sup> proposed to observe QSHE in an inverted InAs/GaSb composite quantum well (CQW), in which the band structure can be tuned with electrical fields<sup>6</sup>, giving rise to a phase transition from a normal insulator to TI via a continuously varying parameter.

In CQW, carriers (electrons and holes) are separated in different wells and the bulk energy gap arises due to the hybridization of the e- and the h- bands at a finite  $k$ -vector in momentum space. This finite  $k$  character is in contrast to that in the HgTe QWs, where the carriers are in the same well and the energy gap opens in the zone center. It is theoretically realized that disorder (which always exists in real materials) could play different roles in the two cases<sup>7</sup> for the experimental observation of QSHE. In this paper we present an experimental study of low-temperature conductivity in mesoscopic size CQW Hall-bar devices. Analyses of our results indicate intricate contributions from the free as well as the hybridized carriers to the bulk CQW conductivity in the presence of a finite amount of disorder. Interestingly, such contributions appear to be independent of the amount of scattering but vary strongly with CQW band parameters<sup>8</sup>.

Transport studies of CQW were reported early by Yang et al<sup>9</sup> and by Cooper et al<sup>10</sup>. In [9] a mini-gap originating from hybridization was observed in capacitance measurements and the density of states (DOS) in the gap regime was analyzed. In [10], the longitudinal resis-

tance  $R_{xx}$  of a larger size CQW Hall bar was measured, observing distinct maxima in  $R_{xx}$  as a function of gate voltage, as the Fermi energy moves through an energy gap at the anti-crossing points of the e- and h- dispersions. Far-infrared measurements<sup>11,12</sup> corroborated the existence of a tunneling-induced mini-gap. These results convincingly show that a mini-gap exists due to e-h hybridization in the inverted regime of InAs/GaSb CQWs. In contrast, a true bulk insulator, which shows temperature activated conductivity has yet to be experimentally confirmed. Moreover, in light of the current interest in observing the QSHE, transport in the mesoscopic-size devices should be measured<sup>4</sup>. Work reported here presents a first experimental study in this direction.

InAs/GaSb CQW was grown by molecular beam epitaxy on silicon-doped  $N^+(100)$  GaAs substrate. The structure consists of a standard buffer consisting of AlSb and  $Al_{0.8}Ga_{0.2}Sb$  layers which accommodates for about 7% lattice mismatch between GaAs and AlSb<sup>13</sup>. On top of this a 500Å AlSb lower barrier was grown, followed by 150Å InAs and 80Å GaSb quantum wells with a 500Å AlSb top barrier and 30Å GaSb cap layer to prevent from oxidation of the AlSb barrier. The sample in which our main results were measured is a Hall bar with width and length of  $0.7\mu m \times 1.5\mu m$  (see inset of FIG. 1c), processed using standard photo- and e-beam lithography techniques with wet etching. The top gate was fabricated by depositing 2500Å  $Si_3N_4$  using plasma enhanced chemical vapor deposition system, and evaporating 1000Å Al or Ti/Au metal gate.  $N^+GaAs$  substrate serves as a back gate for our devices and was contacted using silver resin. Ohmic contacts to the electron-hole layers were made with indium and without annealing. Low temperature magnetotransport measurements were carried out in a  $^3He$  refrigerator (300 mK) combined with a 12T superconducting magnet, or in a  $^3He/^4He$  dilution refrigerator (20 mK) with a 18T magnet (National High Magnetic Field Laboratory). Standard lock-in technique with an excitation current of 100nA at 23Hz was employed.

The energy spectrum of CQW is schematically shown in FIG. 1a. Due to the broken gap alignment of InAs and GaSb, conduction and valence states are confined

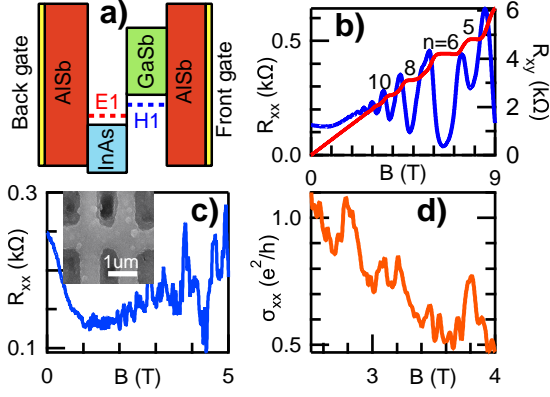


Figure 1: (Color online) a) Shows structure and energy spectrum of inverted CQW with  $E1 < H1$ . Separation of the bands,  $E_{g0}$ , as well as Fermi energy  $E_F$  can be tuned with front and back gates. When  $E_F > H1$ , only electrons are present in the well and representative magneto-transport data at  $T = 0.3$  K is shown in b) for  $10\mu\text{m} \times 20\mu\text{m}$ , and in c) for  $0.7\mu\text{m} \times 1.5\mu\text{m}$  Hall bar (SEM image in the inset) where  $R_{xx}$  exhibits strong fluctuations. d) Fluctuations in conductivity are on the order of  $e^2/h$ , indicating mesoscopic regime.

in InAs and GaSb layers, respectively<sup>14</sup>. For wider wells such as ours, the structure is inverted (FIG. 1a), with the ground conduction subband (E1) lower than the ground heavy-hole subband (H1), resulting in anti-crossing of the bands at a finite momentum value  $k_{cross}$  (FIG. 2a). Assuming that band anisotropy is small, anti-crossing occurs when carrier densities in two wells are equal,  $n = p = k_{cross}^2 / 2\pi$ , corresponding to the resonant condition of equal particle energy and in-plane momentum in two wells. Due to the tunneling induced coupling, electron and hole states are mixed and a mini-gap  $\Delta$  opens in otherwise semi-metallic band dispersion (FIG. 2a)<sup>6</sup>.

In dual gate geometry (FIG 1a), both the relative separation between the subbands,  $E_{g0}$ , and the Fermi energy  $E_F$  can be tuned. When  $E_F$  is between H1 and E1, electrons and holes coexist in their respective layers, resulting in two-carrier transport with characteristic non-linear dependence of Hall resistance on magnetic field<sup>9</sup>. Single carrier transport occurs for  $E_F$  above H1 or below E1, and is electron- or hole-like, respectively. In our CQW,  $E_F$  is pinned by the surface states in the cap layer<sup>15</sup> and under zero applied bias only electrons are present in the well, with a typical low temperature density of  $7 \cdot 10^{11} \text{cm}^{-2}$  and mobility of  $90,000 \text{cm}^2/\text{Vs}$ . Shubnikov de Haas (SdH) oscillations can be observed starting at 1.8T with no evidence of parallel conduction. Hall resistance varies linearly with magnetic field until the appearance of the integer quantum Hall plateaus. A representative trace for electron-like transport in a larger size Hall bar ( $10\mu\text{m} \times 20\mu\text{m}$ ) is shown in FIG. 1b. In contrast, micron-size devices show strong fluctuations in  $R_{xx}$  (FIG. 1c). Fluctuations are reproducible in magnetic field, and conductivity varies on the order of  $e^2/h$

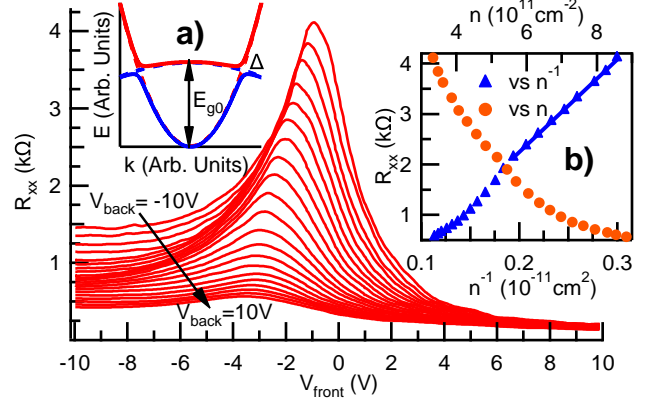


Figure 2: (Color online) Shows  $R_{xx}$  vs.  $V_{front}$  for  $V_{back}$  from 10 to -10 V, in 1V steps,  $B = 0$  T,  $T = 0.3$  K. a) At the anti-crossing point, where  $n = p = E_{g0} \frac{m^*}{\pi \hbar^2}$ , a hybridization gap  $\Delta$  opens. For  $E_F$  in the gap,  $R_{xx}$  exhibits resonance peaks, which decrease for increasing  $V_{back}$ . b) Resonance peaks vary linearly with  $n^{-1}$  for  $n \lesssim 5 \cdot 10^{11} \text{cm}^{-2}$  as proposed in [8].

(FIG. 1d), indicating mesoscopic regime.

In the single carrier regime, electron density changes linearly with front and back bias as approximately  $1.5 \cdot 10^{11} \text{cm}^{-2}/\text{V}$  and  $0.4 \cdot 10^{11} \text{cm}^{-2}/\text{V}$ , respectively. Electron densities are extracted by sweeping gate biases at fixed magnetic field or through analysis of SdH oscillations. Values are consistent and agree well with the parallel capacitor model. When holes are induced in the GaSb well, the effect of front gate on the electron density in the InAs layer is near-perfectly screened. When induced, holes will coexist with electrons in the device bias range and hole density can be extracted by fitting  $R_{xy}$  with two-carrier transport expression. Obtained values are consistent with those for unscreened electrons and in agreement with the parallel capacitor model.

In FIG. 2 we sweep the front bias from 10 to -10 V with the back bias fixed, changing the carriers from solely electrons to predominantly holes, as evidenced from the change of sign in Hall resistance at high magnetic fields. When the carrier densities are matched (i.e.,  $n \sim p$ ), clear peaks in  $R_{xx}$  appear, indicating the existence of a mini-gap. Resonance peaks,  $R_{xx}(max)$ , increase with decreasing back bias, and hence vary inversely with resonance electron-hole density,  $n = p$  and corresponding  $k_{cross}$  (FIG. 2). In particular, for  $n \lesssim 5 \cdot 10^{11} \text{cm}^{-2}$ , resonance peaks vary linearly with  $n^{-1}$  (FIG. 2b). This inverse relationship, which we subsequently discuss, cannot be explained with an increasing mini-gap, for coupling between wells varies proportionally with  $k^{16}$ .

Our central finding is the existence of finite conductivity in InAs/GaAs in the mini-gap regime. Even at the lowest temperature  $T = 20$  mK (FIG. 3a), largest observed resonance peaks  $R_{xx}(max)$  remain  $\leq 5$  k $\Omega$  for mesoscopic samples, which is at least 2-3 times smaller than  $h/2e^2$ . This is in contrast to the case of HgTe QWs

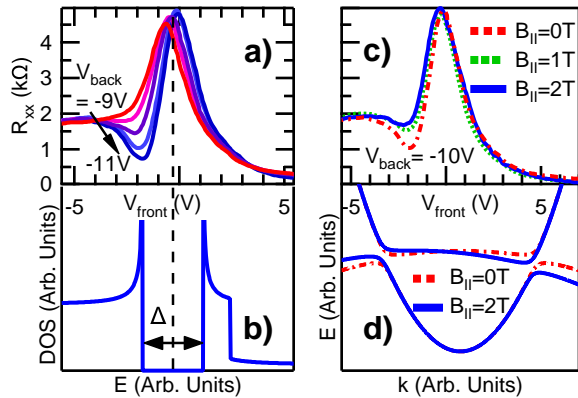


Figure 3: (Color online) a) Shows  $R_{xx}$  vs.  $V_{front}$  for  $V_{back}$  from -9 to -11V, in 0.5 V steps,  $B = 0$  T,  $T = 20$  mK. Resistance dips occur at singularities in DOS near gap edges shown in b). From relative position of dips and peaks in  $V_{front}$  we determine  $\Delta \approx 3.6$  meV. Dips weaken with in-plane magnetic field in c), due to induced anisotropy in the dispersion in d).

where quantized value is approached from larger resistance values<sup>4</sup>. Hence, observed resonance peaks can be understood as a bulk effect, with a residual conductivity on the order of  $10e^2/h$  per square, which is a few times larger than the predicted contribution from the edge. For the remainder of this paper we concentrate on the origin of residual gap conductivity and discuss its implications for the proposed edge modes. We first note that the anisotropy of the heavy hole band may play a role in the gap anisotropy at the Fermi energy, which could lead to residual conductivity. Anisotropy is more apparent for larger  $k_{cross}$ <sup>16</sup> and may explain the decrease of  $R_{xx}(max)$  with larger  $n$  (FIG. 2). To what extent such anisotropy would affect the gap value is a subject for numerical calculations with realistic materials parameters<sup>17</sup>.

Here we show experimentally that band anisotropy plays a minor role in our transport regime. Measurements at  $T = 20$  mK reveal clear dips in  $R_{xx}$  in the vicinity of resonance peaks, for  $V_{back} < -9$  V (FIG. 3a). Such regime corresponds to small on-resonance carrier densities, and observed dips can be explained by van der Hove singularities in DOS (FIG. 3b) at gap edges<sup>16</sup>. In fact, this is the first time that such singularities have been observed in transport, attesting to the high quality of our samples. Resistance dips occur only for smaller  $k$  due to otherwise increasing anisotropy of the valence band, smearing out DOS singularities. Applying in-plane magnetic field (FIG. 3d) induces anisotropy in the direction of the field<sup>9</sup> and dips weaken (FIG. 3c). Thus, at least in the small carrier density regime band anisotropy cannot be responsible for the observed residual conductivity.

We estimate the gap value from the relative position of resistance dips and peaks (FIG. 3a, 3b) in front gate bias as:  $\Delta = 2(V_{peak} - V_{dip}) \frac{\Delta p}{\Delta V} \frac{1}{DOS}$ , where  $\frac{\Delta p}{\Delta V}$  is the rate of carrier density change with front bias, and  $DOS = (m_e + m_h)/\pi\hbar^2$ , with carrier masses  $m_e = 0.03$  and

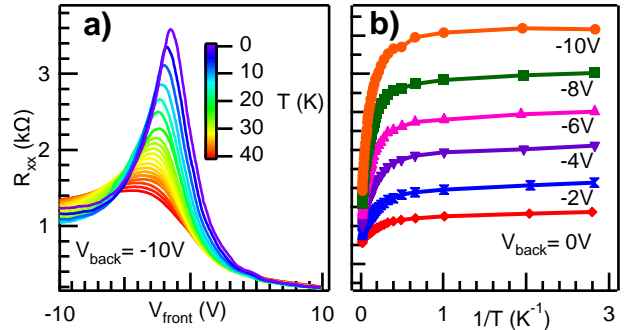


Figure 4: (Color online) a) Shows temperature dependence of resonance peaks for  $V_{back} = -10$  V for  $T$  from 0.3 K to 40 K in roughly 2 K steps. b) Resonance peaks shown vs  $T^{-1}$  saturate for  $T < 2$  K, for six different  $k_{cross}$ .

$m_h = 0.37$  (in units of free electron mass)<sup>9</sup>. We obtain  $\Delta = 3.6$  meV, in agreement with previous studies<sup>9,10,12</sup>. Similar value can be deduced from temperature dependence of resonance peaks (FIG. 4a), which shows insulating character, i.e.  $R_{xx}(max)$  increases in lowering  $T$ . On the other hand, we do not observe temperature-activated resistance, as one would expect for a true insulator. Resonance peaks increase only by a factor of 2-3 over three orders of magnitude change in temperature, for six anti-crossing points measured, and saturate for  $T < 2$  K (Fig. 4b). Nevertheless, peaks persist up to 40 K for all six cases, consistent with a gap value of 3-4 meV.

The lack of gap activation and large residual conductivity suggest that disorder may be important in this system. Hence, we analyze carrier scattering times characterizing the transport in a zero magnetic field. At zero bias, electron scattering time is  $\tau_r = 1.5$  ps and the associated level broadening is  $\Gamma_e = \hbar/2\tau_r = 0.2$  meV. Electron mobility shows linear dependence on electron density and drops to approximately  $40,000$  cm<sup>2</sup>/Vs for the case of smallest electron density of  $3.3 \cdot 10^{11}$  cm<sup>-2</sup>, giving  $\Gamma_e = 0.5$  meV. Linear dependence of mobility on electron density is indicative of short range scattering, presumably from dislocations at interfaces, which is confirmed by extracting the quantum time  $\tau_q$  from SdH oscillations<sup>18</sup>, giving  $\tau_r/\tau_q \approx 7$  at zero bias and validating predominance of large angle scattering. Estimated  $\tau_q$  has been corrected for density inhomogeneity<sup>19</sup> with Gaussian width of  $\delta n \approx 0.35 \cdot 10^{11}$  cm<sup>-2</sup>. On a side note, this suggests that the random potential fluctuations are on the order of  $\delta E = \delta n/DOS \sim 0.25$  meV, and thus  $\delta E \ll \Delta$ . For holes,  $\Gamma_h = b \frac{m_e}{m_h} \Gamma_e$ , where  $b$  is the ratio of electron to hole mobilities. From a fit to  $R_{xy}$  in two-carrier transport regime,  $b \approx 6$ , giving  $\Gamma_h = 0.3$  meV. Thus, total level broadening is less than  $\Gamma = \Gamma_e + \Gamma_h \approx 0.8$  meV, which is a few times smaller than the size of the gap, indicating that disorder may play non-trivial role.

Laikhtman and Naveh<sup>8</sup> have theoretically studied the transport in the inverted regime of InAs/GaAs system,

concluding that even negligible but finite level broadening due to the carrier scattering will result in finite on-resonance conductivity at  $T = 0$  K. Specifically, residual conductivity will go as  $\sigma_{on}(T=0) \sim \frac{e^2}{h} \frac{E_{g0}}{\Delta}$ , when  $\Gamma \ll \Delta \ll E_{g0}$ , thus independent of scattering parameters. Since  $E_{g0} = n \frac{\pi \hbar^2}{m^*}$ , where  $m^* = \frac{m_e m_h}{m_e + m_h}$ , it follows that  $R_{xx}(max) \sim n^{-1}$  as observed in FIG. 2b for  $n \lesssim 5 \cdot 10^{11} \text{cm}^{-2}$ .

The physics of the unusual result in [8] can be understood by re-examining the original premise for carrier hybridization, which is the non-locality of electron states in growth direction of the wells<sup>20</sup>. If this non-locality is suppressed, then hybridization and associated transport properties will be suppressed as well. A natural way for this to happen is through localization of electrons and holes in their respective wells by scattering. Contribution to residual conductivity from such scattered carriers can be quantitatively described within the relaxation time model. The relevant time-scale is carrier tunneling time,  $\tau_t = \hbar/2\Delta$ , and total number of scattered carriers within  $\tau_t$  will go as  $n \cdot (1 - e^{-\frac{\tau_t}{\tau_r}})$ , or equivalently as  $n \cdot (1 - e^{-\frac{\Gamma}{\Delta}})$ . Scattered carriers do not hybridize and contribute to residual conductivity as  $\sigma_{on} \approx \frac{e^2}{h} \frac{E_{g0}}{\Gamma} \left(1 - e^{-\frac{\Gamma}{\Delta}}\right)$ , using that electron mobility is  $\mu_e = \frac{e}{m} \frac{\hbar}{2\Gamma}$  and ignoring smaller contribution from scattered holes. In the limit  $\Gamma \ll \Delta$ , we recover  $\sigma_{on} \approx \frac{e^2}{h} \frac{E_{g0}}{\Delta}$ . Thus, because the number of non-hybridized carriers goes as  $\Gamma$  and their mobility goes as  $1/\Gamma$ , it follows that the bulk conductivity, which is their product, will have constant value independent of  $\Gamma$ .

Besides the contribution to gap conductivity from scattered electrons and holes, Ref. [8] also suggests an ‘‘unusual’’ contribution from hybridized electron-holes, which can be understood as the consequence of non-zero charge of hybridized states due to level broadening. In a two band calculation using independent e- and h- states as a basis<sup>21</sup>, expectation value of this charge can be shown to go as  $\Gamma/\Delta$  for  $\Gamma \ll \Delta$ . Since the mobility varies as

$1/\Gamma$  and the density of hybridized e-h changes slightly, we obtain  $\sigma_{on} \approx \frac{2e^2}{h} \frac{E_{g0}}{\Delta}$ , where the factor of 2 comes from two types of hybridized states. Total conductivity is then  $\sigma_{on} \approx \frac{3e^2}{h} \frac{E_{g0}}{\Delta}$  and from the slope of the linear fit in FIG. 2b we extract the value of the hybridization gap, obtaining  $\Delta \approx 4$  meV – surprisingly close to previous estimates considering the simplicity of the model.

In conclusion, our experiment confirmed the existence of a hybridization-induced energy gap in inverted InAs/GaSb. However, we observed finite bulk conductivity in the gap regime, which can be reasonably explained by the model proposed in [8]. Since the edge modes are only protected by an insulating gap, presence of states inside the bulk gap will allow for scattering of edge states between the opposite sides of the sample, destroying helical transport properties. Nevertheless, an interesting regime for QSHE could exist at the critical point, where the band structure changes from inverted to normal. In contrast to the inverted case, in the normal regime, a real insulating gap exists, and in the vicinity of the critical point, carrier masses can still have opposite signs<sup>6</sup> to those in vacuum due to band repulsion, giving rise to helical edge states. Our work in this parameter regime is in progress.

We thank S.-C. Zhang and D.C. Tsui for bringing our attention to QSHE in InAs/GaAs system, H. Kroemer for invaluable advices on materials, J. Kono, X.-L. Qi, and Kai Chang for very helpful discussions. The work at Rice was supported by Welch Foundation Grant Number C-1682, and a Rice Faculty Initiative Fund. Travel to NHMFL was supported by NSF Grant No. DMR-0706634. A portion of this work was performed at the National High Magnetic Field Laboratory, which is supported by NSF Cooperative Agreement No. DMR-0084173, by the State of Florida, and by the DOE. We thank T. P. Murphy and J. H. Park for expert technical assistance.

\* Electronic address: ik5@rice.edu

<sup>1</sup> C. L. Kane and E. J. Mele, Phys. Rev. Lett. 95, 226801 (2005).

<sup>2</sup> B. A. Bernevig, S. C. Zhang, Phys. Rev. Lett. 96, 106802 (2006).

<sup>3</sup> B. A. Bernevig, T. L. Hughes, S.-C. Zhang, Science 314, 1757-1761 (2006).

<sup>4</sup> M. König, S. Wiedmann, C. Brune, A. Roth, H. Buhmann, L. W. Molenkamp, X.-L. Qi, and S.-C. Zhang, Science 318, 766-770 (2007).

<sup>5</sup> C. Liu, T.L. Hughes, X.-L. Qi, K. Wang, and S.-C. Zhang, Phys. Rev. Lett., 100, 236601 (2008).

<sup>6</sup> Y. Naveh and B. Laikhtman, Appl. Phys. Lett. 66, 1980-1982 (1995).

<sup>7</sup> S.-C. Zhang, private communications.

<sup>8</sup> Y. Naveh and B. Laikhtman, Euro. Phys. Lett., 55, 545-551 (2001).

<sup>9</sup> M. Yang, C. Yang, B. Bennett, and B. Shanabrook, Phys. Rev. Lett., 78, 4613-4616 (1997).

<sup>10</sup> L. Cooper, N. Patel, V. Drouot, E. Linfield, D. Ritchie, and M. Pepper, Phys. Rev. B, 57, 11915-11918 (1998).

<sup>11</sup> J. Kono, B.D. McCombe, I. Lo, W.C. Mitchel, and C.E. Stutz, Phys. Rev. B 55, 1617 (1997).

<sup>12</sup> M. J. Yang, C. H. Yang, and B. R. Bennett, Phys. Rev. B 60, R13958 (1999)

<sup>13</sup> C. Nguyen, B. Brar, C.R. Bolognesi, J.J. Pekarik, H. Kroemer, and J.H. English, Journal of Electronic Materials, 22, 255-258 (1993).

<sup>14</sup> H. Kroemer, Physica E: Low-dimensional Systems and Nanostructures 20, 196-203 (2004).

<sup>15</sup> N. Nguyen, B. Brar, H. Kroemer, and J. H. English, Appl. Phys. Lett., 60, 1854 (1992).

<sup>16</sup> S. de-Leon, L. D. Shvartsman, and B. Laikhtman, Phys. Rev. B, 60, 1861-1870 (1999).

- <sup>17</sup> J. Li, W. Yang, and K. Chang, Phys. Rev. B, 80, 035303 (2009).
- <sup>18</sup> P.T. Coleridge, Phys. Rev. B, 44, 3793–3801 (1991).
- <sup>19</sup> S. Syed, M.J. Manfra, Y. J. Wang, R. J. Molnar, and H.L. Stormer, Appl. Phys. Lett., 84, 1507 (2004).
- <sup>20</sup> A. Palevski, F. Beltram, F. Capasso, L. Pfeiffer, and K.W. West, Phys. Rev. Lett., 65, 1929–1932 (1990).
- <sup>21</sup> G. R. Aizin, B. Laikhtman and G. Gumbs, Phys. Rev. B, 64, 125317 (2001).